Contents

7. Plasma Distribution and Spucecraft Charging Modeling Near Jupiter

Raymond Goldstein and Neil Divine
let Propulsion Laboratory
Pasadena, California

Abstract

To assess the role of spacecraft charging near Jupiter, the plasma distribution in Jupiter's magnetosphere has been modeled using data from the plasma analyzer experiments on Pioneer 10 (published results) and on Pioneer 11 (preliminary results). In the model, electron temperatures are $kT = 4$ eV throughout, whereas proton temperatures range over $100 \le kT \le 400$ eV. The model fluxes and concentrations vary over three orders of magnitude among several co-rotating regions, including, in order of increasing distance from Jupiter, a plasma void, plasma sphere, sporadic zone, ring current, current sheet, high latitude plasma and magnetosheath. Intermediate and high energy electrons and protons (to 100 MeV) are modeled as well. The models supply the information for calculating particle fluxes to a spacecraft in the Jovian environment. The particle balance equations (including effects of secondary and photoemission) then determine the spacecraft potential. Negative potentials the order of 10^3 volts are calculated in the near region (magnetic shell parameter ≤ 6.5 Jovian radii). In the outer region, severe differential charging ($\sim 10^4$ volts) can occur for shadowed, electrically isolated portions of the spacecraft.

This papar presents the results of one phase of research carried out at the Jet Propulston Laboratory, California Institute of Technology, under Contract No, NAN-100, sponsored by the National Aeronautics and Space Administration.

1. INTRODUCTION

Several facts suggest that spacecraft operating in Jupiter's magnetosphere can charge to significant potentials. These include the existence af a highly structured magnetosphere, with novel features compared to the earth's, and known to contain both stable and dynamic populations of thermal and energetic (MeV) electrons and ions. Experience with spacecraft in earth environment, especially at synchronous altitudes, shows that spacecraft charging occurs in such environments, and some ahomalies in the operation of the Pioneer 10 and 11 Spacecraft near Jupiter have been attributed to such charging. The survival and satisfactory operation of a spacecraft orbiting in the Joviah environment is thus of concern, because of the long period of time spend in the severe environment. To assess this problem, environmental models developed from Pioneer data are described below and are applied to preliminary computations of likely spacecraft equilibrium potentials in several magnetosphere regions, in both sunlight and shadow.

2. PLASMA MODEL DEVELOPMENT

The major features of Jupiter's thermal plasma distributions are derived from Prank et al,[1] who present a thorough discussion of the proton component data from the plasma analyzer experiment on Pioheer 10. These data range over values of L (magnetic shell parameter, in Jovian radii R_J) between 2.85 and 25 (within the centrifugally dominated region) and are summarized in their Figure 8. 1 Comparable results from Pioneer 11 are not yet complete but the major additional results are: a plasma viod for $L \leq 1.8$ to 2.0 (within the gravitationally dominated regton), and plasma properties nearly independent of latitude for $L \leq 12$. For high latitudes at $L > 12$, the density is assumed about an order of magnitude smaller than in the current sheet.

For the electron Component more limited results, from Pioneer 10, are discussed by Intriligator and Wolfe,[2] the main conclusion being an electron peak in energy near 4 ev throughout the magnetosphere. Assuming charge neutrality (that is, electron concentrations equal to proton ones) an electron model can b inferred from the above proton distribution.

Ancillary information has been used in the models as follows, in order of increasing distance from Jupiter. Fjeldbo et al,[3] who reports results of Pioneer 10 radio occultations, provlde information which has been used for a very crude specification of the ionosphere; for details of this multilayered environment in Jupiter's upper atmosphere the original reference should be consulted. Near the Galilean satellite Io, the configuration of the atomic hydrogen torus suggests a local proton concentration which ionizes H by charge exchange[4, 5, 6] and the atomic sodium distribution suggests the importance of ionization by local electrons.[7] These results have been used to confirm ar modify the description of the plaema-sphere. Magnetic field data from Ptoneer 10 confirm the reality of the ring current (the source of external field terms For magnetic field modeling,[8] and the proton concentrattoh in the current sheet.[9] Elsewhere various indirect observations and theoretical considerations are generally consistent wtth the foregoing interferences; they include discussions of Faraday rotatton for HF bursts,[10] waveparticle interactions (diffusion, whistlers, etc.),[11, 12, 13, 14] and numerous, primarily qualitative, analyses.[15, 16, 17, 18, 19, 20] A description of the magneto-sheath plasma is taken from considerations of Figure 5 of Wolfe et al.[21]

The present preliminary plasma model should be improved to include aspects of the extended distribution of neutral sodium atoms[7] which is possibly in equilibrium with a sodium ion population. In addition, there are observations of neutral hydrogen,[6] suggesting protoils, and of an ionized sulfur nebula.[22] Other considerations for modification of the model include the character of the 4 eV electron peak seen at large L. This is not clearly thermal In origin and could have been the result of differedtial charging on Pioneer 10.[23] The low energy data From the San Diego scintillators on Pioneer 11[24] should also be included.

3. PLASMA MODEL SPECIFICATION

The plasma distribution derived from the above considerations is specified in Table 1, and the several regions and their boundaries are illustrated in Figure 1.

Values and uncertainties for boundaries and concentrations (equal for electrons and protons) have been estimated. The thermal energy values are quoted without uncertainty because the uncertainties in the distributions which result from the concentration column are already large. In the co-rotating frame (see note (2), Table 1), the thermal distributions are isotropic and may be derived From the entrtes in Table 1 using the following formulae:

$$J_o = 2N_o\left(\frac{2kT}{\pi m}\right)^{1/2} \qquad (1)$$

$$= (1.56 \times 10^6\ cm^{-2}\ s^{-1})\ N_o(kT)^{1/2} \text{ for protons}$$

or

$$= (6.69 \times 10^7\ cm^{-2}\ s^{-1})\ N_o(kT)^{1/2} \text{ for electrons ,}$$

Table 1. Plasma Characteristics for Regions Near Jupiter

Region	Approximate outer boundary	Protons: Characteristic energy, kT, eV	Protons: Flux, J_o, $cm^{-2}s^{-1}$	Electrons: Concentration, N, cm^{-3}	Electrons: Flux, J_o, $cm^{-2}s^{-1}$	Electrons: Characteristic Energy, kT, eV
Ionosphere	$R_J + (-4000\,km)$	0.07	$\le 10^{11}$	$\le 3 \times 10^5$	$\le 5 \times 10^{12}$	0.07
Plasma void	$L = (1.9 \pm 0.1)\,R_J$	100	$\le 10^8$	≤ 10	$\le 10^9$	
Plasmasphere	$L = (6 \pm 0.5)\,R_J$ (Plasmapause and Io flux tubes)	100	$(1.6 \times 2^{\pm 1}) \times 10^9$	$100 \times 2^{\pm 1}$	$(1.3 \times 2^{\pm 1}) \times 10^{10}$	
Sporadic zone	$L = (7.8 \pm 0.5)R_J$	400	$10^8 \times 3^{\pm 1}$	$3 \times 3^{\pm 1}$	$(4 \times 3^{\pm 1}) \times 10^8$	
Ring current	$L = (9.6 \pm 0.5)R_J$ (Europa flux tubes)	400	$(4 \pm 2) \times 10^8$	12 ± 5	$(1.6 \pm 0.7) \times 10^9$	4
Current sheet	$L = (12 \pm 1)R_J$ (1) $Z = \pm(1 \pm 0.5)R_J$	400 (2)	$(3 \times 3^{\pm 1}) \times 10^7$ (2)	$1 \times 3^{\pm 1}$	$(1.3 \times 3^{\pm 1}) \times 10^8$	
High latitude plasma	$R_I = R_M \pm 40R_J$ (3) (Magnetopause)	400 (2)	$3 \times 10^{6 \pm 1}$ (2)	$0.1 \times 10^{\pm 1}$	$1.3 \times 10^{7 \pm 1}$	
Magnetosheath (and tail)	$R_I + 15R_J$ (3)	34 (4)	$(2 \times 3^{\pm 1}) \times 10^7$ (4)	$0.6 \times 2^{\pm 1}$	$(2 \times 3^{\pm 1}) \times 10^8$	34
Interplanetary (solar wind)	Several AU beyond Jupiter's orbit			SEE NASA SP-8118		

Notes: (1) A location is outside the current sheet only if both conditions pertain: $L > (12 \pm 1)R_J$ and $|Z| > (1 \pm 0.5)R_J$

(2) If the speed v relative to the co-rotating plasma exceeds the proton thermal speed, the appropriate entries must be replaced by $mv^2/2$ and Nv for a stationary observer $v = (1.3 \times 10^6\,cm/s)(R/R_J)$ and $E = mv^2/2 = (0.83\,eV)(R/R_J)^2$ dominate for $R \ge 22R_J$

(3) These boundary locations vary strongly with direction from Jupiter [cf. Eq. (6) for R_M] and with time in response to changes in the external solar wind

(4) In the magnetosheath, the variable bulk plasma flow ($v \sim 300$ km/s) dominates the proton thermal speed, so the corresponding flux entry is Nv

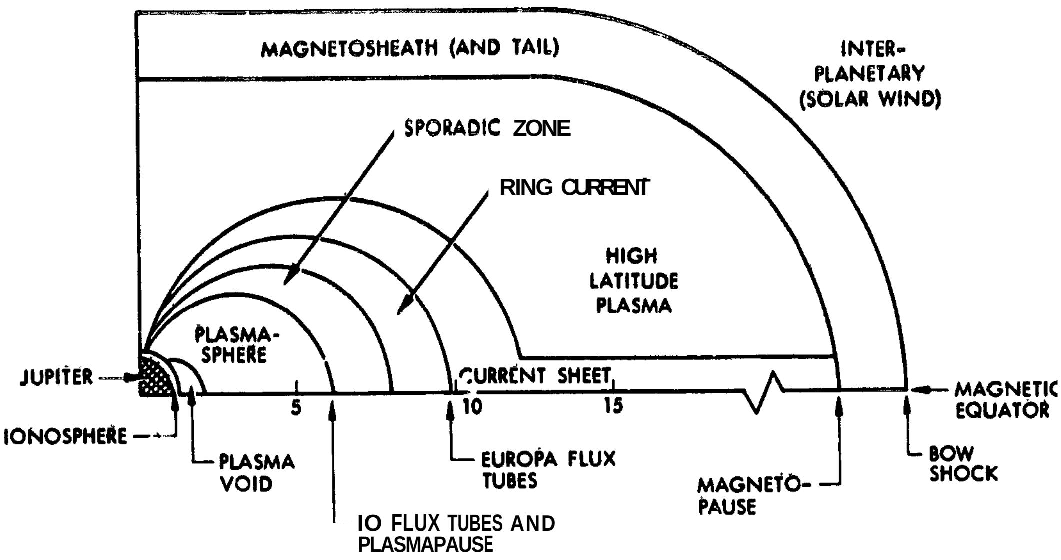

Figure 1. Schematic of Plasma Regions at Jupiter for One Quadrant of a Magnetic Meridional Plane. Drawing is not to scale, although three distances (in R_J) from Jupiter are indicated along the magnetic equator

integral flux (energy > E) $$J = J_o(1 + E/kT)\exp(-E/kT) + J_2 + j_2 (E_2 - E) \quad . \qquad (2)$$

differential flux $$j = J_o E(kT)^{-2} \exp(-E/kT) + j_2 \quad . \qquad (3)$$

In these expressions, values of N_o, J_o, and kT are to be taken from Table 1; in that table, Z represents the vertical distance from the magnetic equatorial plane, and the notes are important. Equations (1) through (3) apply for all thermal and intermediate energies $0 \leq E \leq E_2$ and specify fluxes J and j which are continuous with those in the radiation belt models (see below) when J_2 and j_2 are evaluated at energy E_2, where E_2 = 40,000 eV for electrons and E_2 = 610,000 eV for protons. Care should be taken that energy unit conversions (between MeV and eV) are included when J and j are evaluated in $cm^{-2}\,s^{-1}$ and $cm^{-2}\,s^{-1}\,eV^{-1}$ respectively.

For completeness, in Table 1 reference is made to NASA SP-8118[25] for a description of parameters in the sblar wind.

1. ENERGETIC PARTICLE MODEL

For enorgles exceeding E_2 (see above), there exists a large body of dntn from four energetic charged particle experiments on each of the Pioneer 10 and 11 spacecraft. Because tho literaturo sources and the model specification for this environment are so detatled they will not be described here. The former ore exemplified by several articles In Journal of Geophysical Research, Vol. 79, No. 25 (1974, Sept. 1) and in Science, Vol. 188, No. 4187 (1975, May 2). The model has been developed fer the Jupiter-Orbiter -Probe Study, and has been published for limited distributton,[26] As an example, inner magnetosphere electron flux profiles are shown in Figure 2. The complete radiation belt model includes bbth integral and differential fluxes as functions of position L and λ (magnetic latitude) and particle energy, for both electrons and protons.

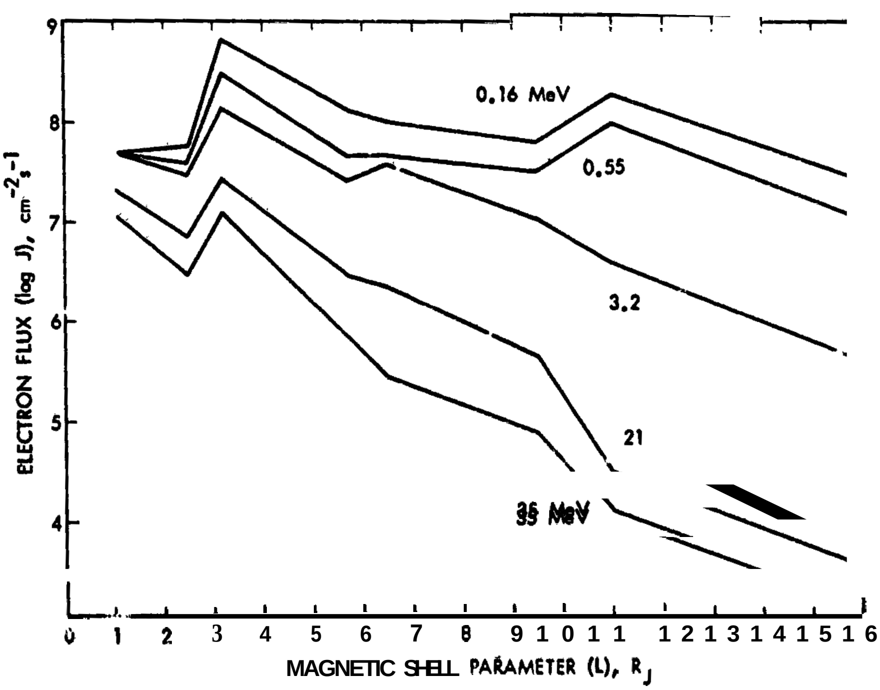

Figure 2. Distance Variation of Equatorial Flux of Electrons Having Energy Greater than the Indicated Threshold Values

5. SPACECRAFT CHARGING CALCULATION

The net current to the spacecraft I_{net} is given by

$$I_{net} = I_p - I_e + I_s + I_{PE} \quad , \tag{4}$$

where I_p is the total protori current intercepted by the spacecraft, I_e is the incident electron current, I_s is the total secondary electron emission from the spacecraft (including backscattered electrons), and I_{PE} is the photoelectron emission current from the spacecraft. Each term is a function of the spacecraft potential $V_{s/c}$ because of the energy dependence of eadh term, At steady state the net current must be zero, establishing the condition €or determining $V_{s/c}$. If Equation (4) is divided by the appropriate area, this condition can be expressed in terms of particle fluxes. It is assumed that essentially all of the spacecraft is covered with electrically conductive material, and that on the average, only 25 percent of the surface is exposed to sunlight, Then the condition for zero net current becomes

$$J_p(V_{s/c}) - J_e(V_{s/c}) + J_s(V_{s/c}) + J_{PE}(V_{s/c}) = 0 \quad . \tag{5}$$

The J's represent the particle fluxes of the corresponding terms of Eq. (4); and the dependence on $V_{s/c}$ is explicitly shown for emphasis. To normalize the photoelectric term properly, a factor 0.25 is implicitly included in J_{PE}.

Equation (5) was used to calculate $V_{s/c}$ at various locations in the Jovian magnetosphere using values of J_p and J_e provided by the model described in the previous sections. The results of Sternglass for aluminum, as reported by Whipple,[27] were used to calculate J_s. Whipple's value of photoelectron yield for aluminum at 1 AU (3×10^{-9} A cm^{-2}) reduced for 5.2 AU, was used to determine J_{PE}. Although most spacecraft are not likely to be covered with aluminum, the yields were taken to be typical of conductive materials.

The calculations were performed by assuming a $V_{s/c}$ and then iterating until a self-consistent value could be obtained. Usually a rapid convergence of the calculatioh was obtained with very few iteratiohs. Thte is largely due to the dependence of the secondary emission yield on incident proton energy. Below about 10^3 eV the yield is much less than unity, but above 163 eV the yield rtses very rapidly with energy exceedtng unity at about 2 X 103 eV. Thts raptd increase in yield with energy produces a htgh sensitivity of the calculatton to $V_{s/c}$ since all low energy protons are accelerated by a negattve spacecraft potenttal. The high secondary yield thus tends to limit negattve spacecraft potentials to a few keV in regions of the mognetosphere where photoemission is unimportant.

6. RESULTS AND DISCUSSION

The contribution of each term of **Eq. (5)** at the steady state spacecraft potential for several locations in the **Jovian** equatorial plane is shown in Figure 3. The calculated spacecraft potentials are also given. The lower part shows the incident electrdn current density, In the upper part of the figure, the proton as well as secondary and photbemission contributions ard shdwn. Note that for $L \leq 6.5\ R_J$ photoemission is riot every important. For higher L, however, photoemission begins td dominate arid the spacecraft charges to a slight positive potential. In those cases the actual secondary and photoemission contributions depend on details of their energy distributions, and for simplicity sere not calculated in detail, Their sum is thus shown in Figure 3 for $L \geq 9.5\ R_J$.

The inciderit electron current density Corresponding to the $V_{s/c}$ calculated at steady state is indicated by the light horizontal line shown in the electron contribution? separating two differently shaded regions. The **full** column Pepresents the total $J_e(0)$ that would occur if the **poteritial were** zero, arid hence the doubly **cross**-hatched region corresponds to that portion of the electrori spectrum repelled by the spabecraft to produce the current balance.

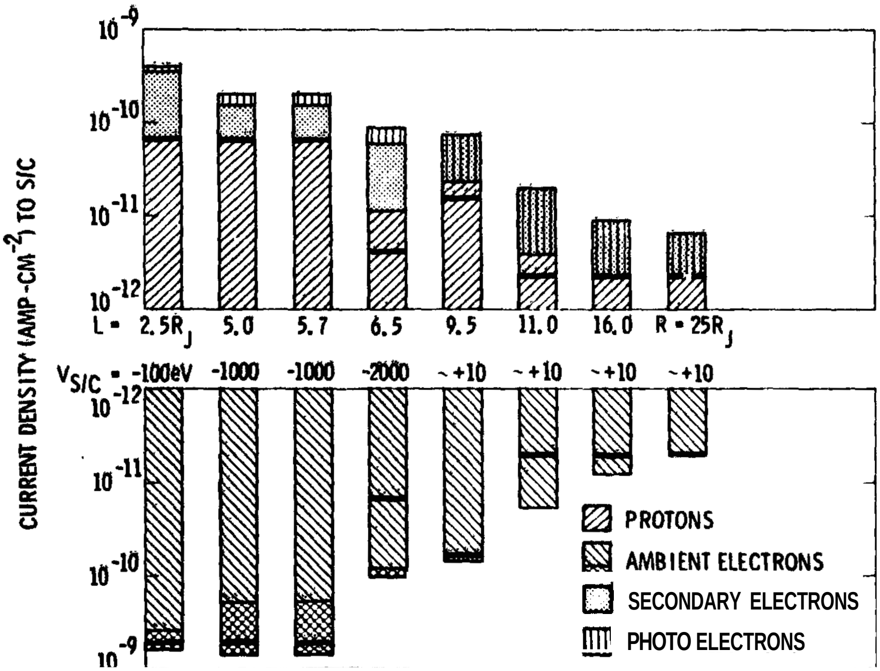

Flgure 3, Distribution of Particle Fluxes tö and From Spacecraft in Jovian Equatorial Plane

The heavy horizontal line appearing in each column shows the relative contribution to the tbtal ihcident flux due to low energy plasma particles and high energy particles, In each case the plaema contribution is the portion closest to the center of the figure.

Calculations were also carried out neglecting the photoemission term, that is, for a spadecraft in eclipse. In the inner region, where photcetnission is unimportant (cf. Figure 3), potentials for the dark case are not very different from the sunlit case. However, in the outer regions where photoemission is important, relatively high potentials are calculated for a spacecraft in darkness. The potentials for both the sunlit as well as eclipse cases are summarized in Table 2. Also shown there are the potentials calculated for ode point in the high latitude region ($L = 16.0\ R_J$, $\lambda = 45^o$). In the outer regions total eclipse of the spacecraft is unlikely, but the eclipse potentials indicate the level to which electrically isolated portions in darkness are likely to charge.

Some calculations were also performed to determine the sensitivity of the results to the fraction of the spacecraft assumed to be in Sunlight. In the inner region this is not too important, but in the outer region a 10 percent sunlit spacecraft would have a negative (10^2 - 10^3) potential.

Table 2. Calculated Spacecraft Patentials in the Jovian Environment

Location	V_{sc} Sun (volts)	V_{sc} ECL (volts)
$L = 2.5\ R_J$	-100	-200
5.0	-1000	-1500
5.7	-1000	-1500
6.5	-2000	-3500
9.5	~ +10	~ +10
11.0	~ +10	-10^4
16.0	~ +10	-1500
16.0, $\lambda = 45^o$	~ +10	-10^4
$R \approx 25\ R_J$	~ +10	-10^4

7. SUMMARY AND CONCLUSIONS

A model of the Jovian charged particle environment has been constructed from results of Pioneer 10 and 11 measurements. This model was used to calculate the potential to which .a spacecraft would charge in the Jovian environment. In the inner region ($L \leq 6.5\ R_J$), the potentials calculated ($\sim 10^3$ volts negative) indicate severe disturbances to fields add particles measurements from the spacecraft. "Clean" measurements would therefore require active control of the spacecraft potehtial. In the outer regions, electrically isolated portions of the spacesraft are likely to charge differentially $\sim 10^3$-10^4 volts with respect to sunlit portions. High differential charging seriously distorts fields and particles measurements, and represents sources for arcing severe enough to damage the spacecraft or cause malfunction.

References

1. Frank, L.A. et al (1976) Observations of plasmas in the Jovian magnetosphere, J. Geophys. Res. 81(No. 4):457-468.
2. Intriligator, D. S., and Wolfe, J. H. (1974) Initial observations of plasma electrohs from the Pioneer 10 flybp of Jupiter, Geophys. Res. Letters 1(No. 7):281-284.
3. Fjeldbo, G. et al (1975) The Pioneer 10 radio occultation measurements of the ionosphere of Jupiter, Astronomy and Astrophpsics 39(No. 1):91-96.
4. McDonough, T. R. (1975) A theory of the Jovian hydrogen torus, Icarus 24 (No.4):400-406.
5. Carlson, R. W., and Judge, D. L. (1974) Pioneer 10 ultraviolet photometer observations at Jupiter encounter. J. Geophys. Res. 79(No. 25):3623-3633.
6. Carlson, R. W., and Judge, D. L. (1975) Pioneer 16 ultraviolet photometer observations of the Jovian hydrogen torus: the angular distribution, Icarus 24(No. 4):395-399.
7. Carlson, R. W. et al (1975) Electron impact ionization of Io's sodium emission cloud, Geophys. Res. Letters 2(No. 10):469-472.
8. smith, E. J. et al (1976) Jupiter's magnetic field and magnetosphere, in Jupiter, University of Arizona Press, Tucson, pp. 788-829.
9. Smith, E. J. et al (1974) The planetary magnetic field and magnetosphere of Jupiter: Pioneer 10, J. Geophys. Res. 79(No. 25):3501-3513.
10. Goertz, C. K. (1974) Polarization of Jovian decametric radiation, Planetary and Space Sci. 22(No. 11):1491-1500.
11. Scarf, F. L., and Sanders, N. L. (1976) Some comments on the whistler mode instability at Jupiter, J. Geophys. Res. 81(No. 10):1787-1790.
12. Barbosa, D. D., and Coroniti, F. V. (1975) Whistler stability analysis in Jupiter's inner. radiation belt, AGU Trans. EOS 56(No. 12):1041.

13. Sentman, D. D. et al (1976) Plasma densities in the inner Jovian magnetosphere, AGU Trans. EOS 57(No. 4):316.

14. Eviatar, A., and Ershkovich, A. I. (1976) Plasma density in the outer Jovian magnetosphere, J. Geophys. Res, 81(No. 22):4027-4028.

15. Hill, T. W. et al (1974) Configuration of the Jovian magnetosphere, Geophys. Res. Letters 1(No. 1):3-6.

16. Barish, F. D., and Smith, R.A. (1975) An analytical model of the Jovian magnetosphere, Geophys. Res. Letters 2(No. 7):269-272.

17. Prakash, A., and Brice, N. (1975) Magnetospheres of Earth and Jupiter after Pioneer 10, Space Sci. Reviews 17(No. 6):823-835.

18. Roederer, J. G. (1976) Planetary plasmas and fields, AGU Trans. EOS 57(No. 2):53-62.

19. Goertz, C.K. (1976) The current sheet in Jupiter's magnetosphere, AGU Trans. EOS 57(No. 3):155.

20. Goertz, C. K. (1976) Plasma in the Jovian Magnetosphere, J. Geophys. Res. 81(No. 13):2007-2014.

21. Wolfe, J. H. et al (1974) Pioneer 10 observations of the solar wind interaction with Jupiter, J. Geophys. Res. 79(No. 25):3489-3500.

22. Brown, R.A. (1976) A model of Jupiter's sulfur nebula, Astrophys. J. 206(No. 3):L179-L183.

23. Grard, R. J. L., DeForest, S. E., and Whipple, Jr., E. C. A reinterpretation of low energy electron measurements in the Jovian magnetosphere, J. Geophys. Res. in press.

24. Fillius, R. W., McIlwain, C. E., and Mogro-Campero, A. (1975) Radiation belts of Jupiter: a second look, Science 188(No. 4187):465-467.

25. Divine, N. (1975) Interplanetary Charged Particle Models (1974), NASA SP-8118.

26. Divine, N. (1976) Jupiter Charged-Particle Environment for Jupiter Orbiter Probe 1981/1982 Mission, Document 660-24, Jet Propulsion Laboratory, Revised August 1976.

27. Whipple, E. C., Jr. (1965) The Equilibrium Electric Potential of a Body in the Upper Atmosphere and in the Interplanetary Space, NASA Technical Note X-615-65-296.